

Metal Organic framework as drug delivery platform

Swati Raysing*, Sumit Pode*,

Department of Quality Assurance & Industrial Pharmacy R.C. Patel Institute of Pharmaceutical Education and Research, Shirpur 425405, Maharashtra State, India

Submitted: 15-07-2023

Accepted: 25-07-2023

ABSTRACT:Theranostic applications have showed considerable promise for metal-organic framework (MOF) nanoparticles as carrier platforms. Different tactics have been created to get around the drawbacks of conventional pharmaceutical therapy. The hydrophilicity of pharmaceuticals can be changed by using nanoparticles as drug delivery devices to impact drug absorption and efflux in tissues. They promote medication accumulation at the sites of the lesions and prevent pharmaceuticals from non-specifically binding with bio-macromolecules, enhancing therapeutic efficacy and minimizing unneeded side effects. MOFs' variable porosity structure and adaptable chemical makeup allow for the engineering and improvement of their medical formulation and functionality as useful carriers for either therapeutic or imaging agents. The review provides the most recent updates for the above-mentioned subjects as well as information on the toxicity of MOFs for human usage. In relation to translational medical research, the problems and opportunities that NMOFs may face in the future are also explored. To create clinically applicable NMOFs for various nanomedicine applications, further work needs to be done.

KEYWORDS: Metal organic framework, nanocarriers, drug delivery, bioMOFs, Advanced therapies.

I. INTRODUCTION

The wide range of active ingredients (AIs) available today all have low therapeutic efficacy due to related limitations as rapid biodegradation, instability, low treatment specificity, systemic side effects, and toxicities. Additionally, several AIs have a restricted solubility, which frequently causes the emergence of multidrug resistance (MDR) following a protracted course of therapy. Due to these restrictions, administering bioactive molecules to patients necessitates the creation of new techniques to ensure their precise transport, their prolonged release over time, and at a controlled rate, thereby lowering side effects and boosting

therapeutic efficacy. By preventing biological compensation, limiting doses for each component, or accessing context-specific multi-target mechanisms, a combination of two or more medicines can overcome the toxicity and other adverse effects brought on by high doses of a single treatment [1–3]. Additionally, simultaneous diagnosis, therapy, and therapeutic response monitoring are made possible by the integration of diagnosis and therapy in one system [4]. In this situation, the development of multivalent drug-delivery systems (DDS) has been facilitated by the design of combined treatments. Basically, DDS basically work around some of the shortcomings of traditional treatments. DDS is a formulation that regulates the dose, duration of release, and effect of an active or imaging agent in a particular region of the body.

A brand-new category of extremely adaptable hybrid materials called metal-organic frameworks (MOFs) is made up of metal bridging ligands and organic bridging sites [5]. They are also known as coordination polymers or coordination networks, and they are normally synthesized under benign conditions using coordination-directed self-assembly processes (Figure 1) [6–10]. For various applications, including nonlinear optics, gas storage, catalysis, and chemical sensing, MOFs are well explored by the scientific community due to their enormous porosity and variable pore sizes, shapes, and functionalities [5,6,9–16]. Due to their exceptionally high surface areas and large pore sizes for drug encapsulation, intrinsic biodegradability as a result of their relatively labile metal-ligand bonds, and versatile functionality for post-synthetic grafting of drug molecules, MOFs exhibit many desired characteristics as drug carriers. For use in the loading and release of various pharmacological compounds, MOFs have been researched over the past three years. Several methods that have been established for inorganic and organic polymeric nanoparticles can be used to scale down MOFs to the nano domain to create nanoscale metal-organic frameworks (NMOFs). NMOFs are prospective

nano vectors for the delivery of therapeutic medicines to specific regions of the body because they have large surface areas, high porosities, and functional groups that can interact with loaded moieties to control drug release. Recently, our team revealed MOFs as significant contrast agent delivery systems for optical, computed tomography, and magnetic resonance imaging [17-21]; However, the uses of MOFs and NMOFs as possible drug carriers will be the main emphasis of this review. Although they are still in their infancy, NMOFs show a variety of desirable properties as nanocarriers; their inherent tunability and biodegradability, as well as their exceptionally high drug loading capacity, should make them a promising candidate for further research and development as nanotherapeutics.

II. SYNTHESIS OF MOFS

For the purpose of producing MOFs with the desired size, surface topology, chemical composition, and application area, a variety of synthetic methods have been proposed. The form and surface morphology of MOFs are often tuned by the MOFs, which in turn depends on a number of other parameters. We'll talk about several MOF synthesis techniques as well as alternate approaches used to modulate and adjust MOF form. Fig. 2 gives an overview of different types of MOFs along with the synthesis methods.

2.1. Conventional synthesis methods: These synthesis techniques rely on the use of heat to create MOFs. The type of MOFs being made once depended heavily on the temperature. These processes were classified as solvothermal or non-

solvothermal syntheses depending on the environment in which they were carried out. While non-solvothermal synthesis uses solvents with boiling points higher than those of solvothermal synthesis, solvothermal synthesis often uses water as the solvent. The non-solvothermal approach requires no complicated reaction setup and is simple to use. This approach has been used to synthesize several MOFs. Specifically, simple solution mixing without heating produced MOF-5, MOF-74, MOF-177, HKUST-1, and ZIF-8. On the other hand, solvothermal synthesis is advantageous for the synthesis of crystalline MOFs. Higher yields are produced, and the product has superior crystallinity. A high yield and the creation of crystals with regular spacing are the results of reaction conditions, such as higher pressure, which warms the solvent and increases the solubility of the precursors. The non-solvothermal approach has also been utilized to create MOF UiO-67 utilizing DMF as the solvent, $ZrCl_4$ as the linker, and terephthalic acid as the linker. It demonstrated the greatest MOF degradation temperature of $540^\circ C$ [22–26]. The standard way of synthesis is pretty helpful, but in the case of non-solvothermal methods, the choice of solvents is extremely important since it affects not only the shape and size of MOFs but also their toxicity, which is covered in more detail later in the article. Designing MOFs for catalysis can benefit from the high yield and creation of uniformly spaced crystals advantages. In a non-solvothermal method, optimizing the solvent choice will aid in maintaining a balance between the synthesis of MOFs with the appropriate quality attributes and their toxicity



Fig no.2.1 Conventional synthesis method

2.2. Microwave-assisted synthesis of MOFs

The conventional methods for the synthesis of MOFs are frequently laborious and involve lengthy reactions. This technique was developed to address this difficulty and synthesize MOFs in shorter time periods. The choice of

solvent is the one limitation of this process above conventional techniques. In both solvothermal and non-solvothermal processes, the boiling point of MOFs was evaluated before selecting a solvent; however, in microwave-assisted MOF synthesis, the solvent is selected based on its microwave

absorption ability (Fig No.2.2). The microwave absorption ability of the solvent determines its ability to transform electromagnetic energy into heat to aid the reaction. The reaction vessel is the second need for starting microwave aided synthesis of MOFs because the penetration depth varies with temperature. As a result, for efficient heating in a microwave oven, either use a large enough container or mix the cooked sample. In 2005, the first MOFs were created via microwave radiation-based synthesis. With the help of microwave radiation, the reaction time of MOFs such as MIL-100 was reduced from 96 hours to 4 hours using H3BTC as the precursor and an aqueous solution of hydrofluoric acid. While MIL-100 was totally created in one hour, chromium took four hours to completely disappear [27].

MIL-101 ($\text{Cr}_3\text{F}(\text{H}_2\text{O})_2\text{O}[\text{C}_6\text{H}_4(\text{CO}_2)_2]_3$) was also synthesized utilizing microwave radiation and terephthalate as a linker. The contamination was entirely eliminated after exposing the material to radiation for at least 60 minutes. It has been shown that the particle size of MIL-101 varies with irradiation time. After 15 minutes of irradiation,

MOFs with a size of 50 nm were produced. In a comparable work, instead of terephthalate, amino-terephthalic acid was used as a linker to manufacture MIL-101 utilizing microwave energy. Within 5 minutes of microwave irradiation, Fe-MIL-101-NH₂ MOFs of 200 nm were formed. According to the available literature, irradiation period, linker type, and power may all play a role in defining the particle size of synthesized MOFs. [28–34]. HKUST-1 was synthesized using this method. We can clearly conclude from the foregoing discussion that the microwave synthesis approach will help shorten the time needed for the synthesis of MOFs, but at the same time, this method might not be useful for MOFs that contain proteins as either the core or the shell of their composition. Depending on the intensity and duration of the radiation, the particle size can be changed. This can be utilized to create core-shell MOFs, where the core serves as a surface on which MOFs can seed their structure. Nevertheless, there haven't been many reports on the synthesis of core-shell MOFs with a unique, non-MOF core. You can investigate this technique for the same.

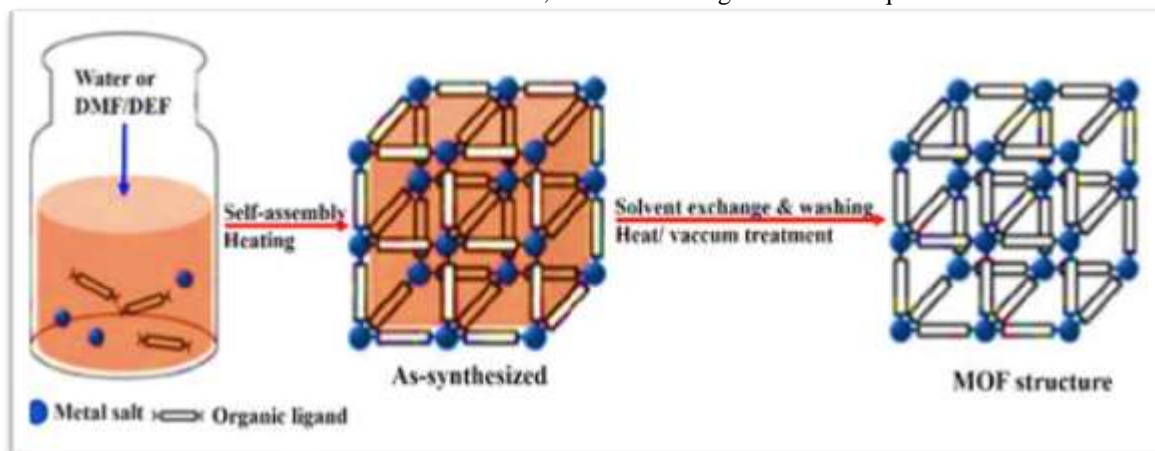


Fig no.2.2 Microwave-assisted synthesis of MOFs

2.3. Electrochemical synthesis

This method of MOF synthesis is based on the supply of metal ions as the anode while the linker molecule is dissolved in reaction mixture along with electrolyte. This approach can be used to produce MOFs indefinitely. The use of protic solvents in the reaction mixture prevents metal ion deposition from the anode onto the cathode (Fig. 4). In a similar study, it was established that the hydrothermal approach, non-solvothermal method, and electrochemical method of synthesis all yield $\text{Cu}_3(\text{BTC})_2$ phases with nearly identical pore volumes and surface area of HKUST-1 MOFs [35].

BASF reported an electrochemical synthesis approach of MOFs to eliminate anions such as chloride, perchlorate, and nitrate during large-scale manufacture. This approach was used to synthesize a variety of anode combinations including zinc, copper, magnesium, and cobalt with linkers such as 1,3,5-H₃BTC, 1,2,3-H₃BTC, H₂BDC, and H₂BDC-(OH)₂. Copper and zinc-based compounds with high porosity were produced from these combinations [36]. Other MOFs structures have been tried in addition to MOFs nanoparticles and porous nanoparticles. Patterned coating and film have been prepared using HKUST-1. The growth

of film was mediated by controlling the reaction conditions carefully [37]. For the synthesis of MOFs, the galvanic replacement approach was used as an alternative to the traditional electrochemical method. Using metallic Cu placed on a glass slide, a layer of tiny octahedral crystallites with particle sizes ranging from 100 to 200 nm was created. Silver ions oxidized copper during the spin-coating of H₃BTC, DMSO, and AgNO₃ on a copper-coated glass slide, resulting in

the creation of octahedral HKUST-1 crystallites [38]. Previously, electrochemical synthesis methods were investigated for the creation of porous metal nanoparticles such as platinum and platinum base alloys. This method of synthesis of MOFs can be paired with porous metal nanoparticles to create a novel class of porous core-shell MOFs that can be investigated further for catalysis or drug delivery.

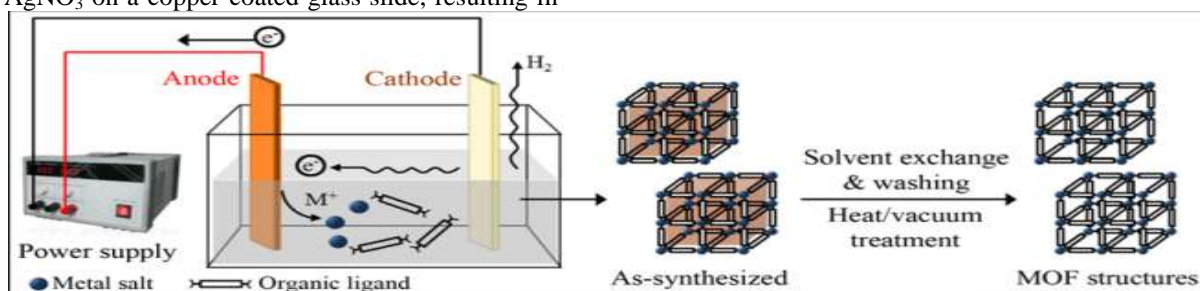


Fig. No.2.3 Electrochemical synthesis

2.4. Sonochemical synthesis

Sonochemical synthesis is the application of high-energy ultrasound to a reaction mixture. The Sonochemical technique of synthesis is very new, with only a few MOFs produced using it, including MOF-5, MOF-177, and HKUST-1 [39-40]. An aqueous solution of zinc acetate and metal, as well as H₃BTC as a linker, was combined and ultrasonicated at room temperature to create [Zn₃(BTC)₂] MOFs in a MOFs synthesis utilizing Zn carboxylates [41]. When compared to the solvothermal technique of synthesis, this procedure was faster. Similarly, MOF-5 crystals were grown in a horn-type reactor using NMP as a solvent [42]. The duration of the reaction was 30 min. MOF-5 crystals have also been reported to be made using the same procedure but with DMF as the solvent instead of NMP [43]. In the case of HKUST-1,

copper acetate was combined with H₃BTC in a DMF, ethyl alcohol, and water solution. MOFs with particle sizes ranging from 10 nm to 40 nm were produced under the reaction conditions of ultrasonication time and strength. With increasing reaction time, MOF particle size increased, resulting in the creation of MOFs ranging in size from 50 nm to 200 nm. Aside from an increase in particle size of MOFs, deterioration of MOFs was detected with an increase in reaction duration, as evidenced by hazy TEM images of HKUST-1 with irregular form and morphology [43-45]. The concentration of DMF influenced the particle size and uniformity of MOFs. Instead of DMF, H₃BTC was combined with NMP in another MOF-177 synthesis. The reaction lasted 40 minutes and produced MOF-177 crystals with particle sizes ranging from 5 to 50 nm [46].

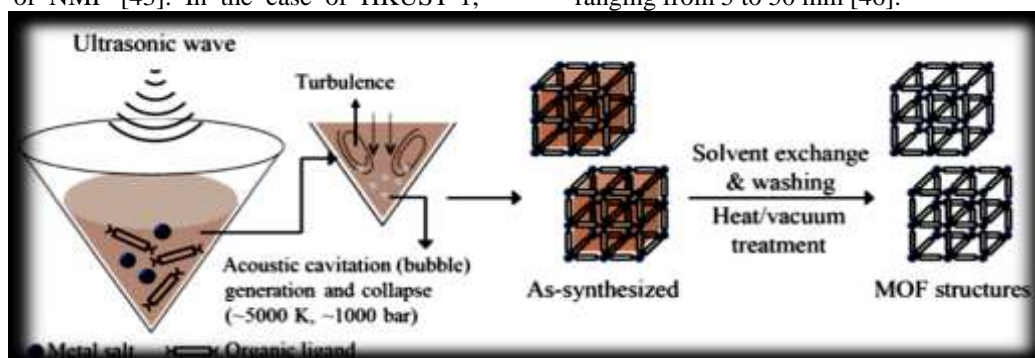


Fig no.2.4 Sonochemical synthesis

2.5. Mechanochemical synthesis

The term "mechanochemical synthesis" refers to the use of mechanical energy in the reaction. Mechanical breaking of intramolecular bonds occurs, followed by a chemical transition. The benefits of mechanochemical synthesis include the ability to perform it at room temperature and without the use of a solvent [47]. Aside from the advantages of a quick reaction time, low temperature, and solvent-free synthesis, this method allows you to use metal oxide salts as a precursor instead of metal salts, which produce just water as a by-product. Due to their low solubility in solvents, metal oxide-based precursors are often not employed; thus, only mechanochemical

synthesis methods are suitable in the case of metal oxide salt precursors, such as in the instance of pillared-layered MOFs and ZIFs involving zinc, where zinc oxide was used as a precursor [48,49]. In a few circumstances, a little amount of solvent is added to help speed up the mechanochemical reaction, which is known as liquid aided grinding (LAG) [50,51]. LAG has structure-directing capabilities in addition to speeding up the reaction. ILAG (ion and liquid assisted grinding), like LAG, was discovered to be highly efficient for the selective building of pillar Layered MOFs [52]. This approach has also been used to synthesis many additional MOFs, including HKUST-1 and Cu (INA)₂.

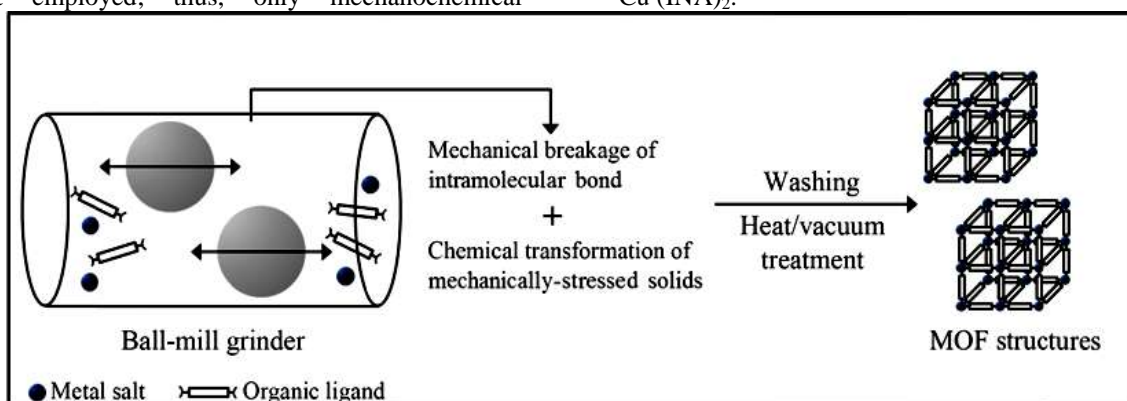


Fig no. 2.5 Mechanochemical synthesis

III. BIODEGRADABILITY AND STABILITY OF MOFs

The stability of MOFs is another heated topic for their use in drug delivery system. A certain degree of chemical instability of the matrix's substance is regarded desirable for medicinal applications since it can disintegrate in situ and the degradation products can be dealt with by the body's own systems, preventing endogenous build-up. Furthermore, the degradability of MOFs allows drugs to diffuse from matrix materials, boosting drug release efficiency, albeit this performance is also controlled by host-guest interactions, pore size, and hydrophobic/hydrophilic characteristic [53]. However, proper matrix material stability is still necessary to ensure the solids' integrity before completing their functions. For example, as an anticancer medication carrier, the matrix's substance is intended to retain its structure before reaching the tumor tissue. So far, relatively little information has been acquired regarding the stability of MOFs in real body liquid, while the stabilities of various MOFs, such as MIL-100(Cr),

MIL-101(Cr), MIL-53(Cr), and Zeolitic Imidazolate Framework-8 (ZIF-8), have been examined under simulated physiological settings. MIL-100(Cr) is a 3D mesoporous material with a trimeric metal octahedron and 1,3,5-tricarboxybenzene (BTC) structure. The major degradation of it was observed after three days under simulated body fluid. MIL-101(Cr) was synthesized utilizing the same Cr trimeric and terephthalic acid, resulting in a zeotype cubic structure that deteriorated after 7 days in simulated bodily fluid (SBF) at 37°C [54]. MIL-53(Cr) is a 3D framework made of terephthalate (BDC) and Cr octahedron trans-chains with a 1D pore channel system. In SBF, the primary deterioration occurred until 21 days [55]. ZIF-8, which is formed of ZnN₄ tetrahedra linked by imidazolate anions, is highly hydrothermally stable and retained its structure after 7 days suspended in PBS (phosphate buffered saline, pH 7.4) at 37°C [56]. However, it has reduced stability in acetate buffer (pH is at 5.0, approximated physiological conditions of tumor tissue) and degrades quickly within a few minutes. This is due in part to the fact that the imidazolate linker is more easier to protonate in acetate buffer,

which reduces the linker's complexing potency toward metals. These findings reveal that the stabilities of MOFs are substantially influenced by their composition, crystalline structure, and external circumstances. Thus, tweaking these factors could result in acceptable MOF stability. However, a rigorous investigation of MOF stability in vivo is still required to better understand their function in organisms.

IV.COMBINED ADVANCED DRUG DELIVERY THERAPIES

Research efforts are focused nowadays in the development of nanotechnology-based delivery systems for efficient treatment of several diseases. As mentioned in the introduction, different platforms have been used as drug host materials (mesoporous silicas, liposomes, zeolites, MOFs), taking advantage of different administration routes and cell uptake mechanisms (endocytosis vs.

membrane diffusion) to provide more targeted systems, improving their stability and pharmacokinetics. In this paper, we review the key techniques and integrated advanced therapies that have been reported in the literature using MOFs as DDS in conjunction with: bioMOFs, other pharmaceuticals, biomolecules (proteins, ribonucleic acid (RNA)), metals, and therapeutic gases. Taking into account all of the available options, this section proposes categorizing MOFs for combined advanced therapies based on the nature of the active components, beginning with a bioactive framework with an incorporated drug and progressing to MOFs with two drugs, drug and biomolecule, drug and active metal, and drug and bioactive gas. Although co-encapsulation of two or more AIs in the same MOF has been proposed as a platform in theragnosis, this will be covered in a later section, leaving this section to explore integrated advanced therapeutics.

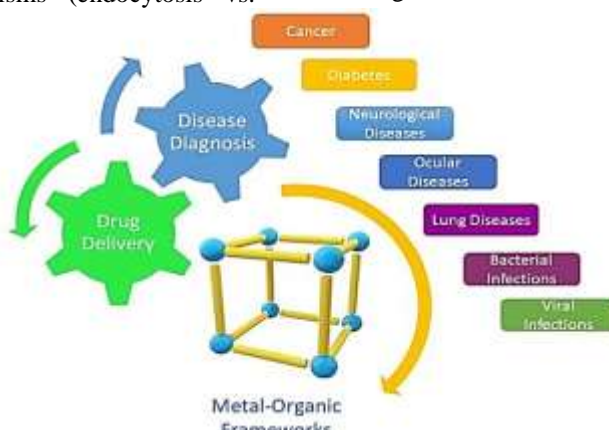


Fig. No. 4 Combined advanced drug delivery therapies

4.1. Drug-bioactive MOF therapy: following synthetic modification Some of the main intrinsic properties of MOFs, such as compositional versatility, exceptional porosity, tunable crystal size, and surface chemistry [57], have led researchers to use them in biological applications such as the delivery of AIs such as drugs, biomacromolecules, metals, and gases, among others. AIs can be incorporated into MOFs in several ways: i) as a constitutive part of the hybrid network (BioMOF), ii) inclusion of AIs in the MOF porosity (via diffusion methods or direct in situ synthesis, pursuing the AIs@MOF core@shell formation, and iii) interaction of the AIs with the MOF external surface due to different forces (e.g., covalent bond, hydrogen bond) [58,59].

4.1.1. Combined therapy based on BioMOFs

AIs might be directly included into the MOF network as building units (BUs), ligands, and/or metallic clusters, allowing AIs to be delivered using the MOF breakdown process in physiological fluids. BioMIL-1 ($\text{Fe}_2^{\text{III}}\text{Fe}_{1-x}^{\text{III}}\text{Fe}_x^{\text{II}}\text{O}(\text{OH})_y[\text{O}_2\text{C}-\text{C}_5\text{H}_4\text{N}]_5[\text{O}_2\text{CCH}_3]$, $x = 0.15$; crystal size: $0.2 \times 0.2 \times 0.1$ mm) prepared with nontoxic Fe^{3+} and nicotinic acid (vasodilating and antilipemic drug) is released within one hour under physiological simulated conditions (pH = 7.4, 37°C) [60], BioMIL-5 ($\text{Zn}(\text{C}_9\text{O}_4\text{H}_{14})$, crystal size: 5-10 mm), a combined DDS based on azelaic acid (antimicrobial and anti-inflammatory properties) and Zn^{2+} (endogenous transition metal, commonly used in dermatology) with antimicrobial activity against Gram (+) *Staphylococcus epidermis* and *S. aureus* [61]. While these bioMOFs provide a

significant chance for combination therapies as hosts for other AIs, there are few examples in the

literature so far.

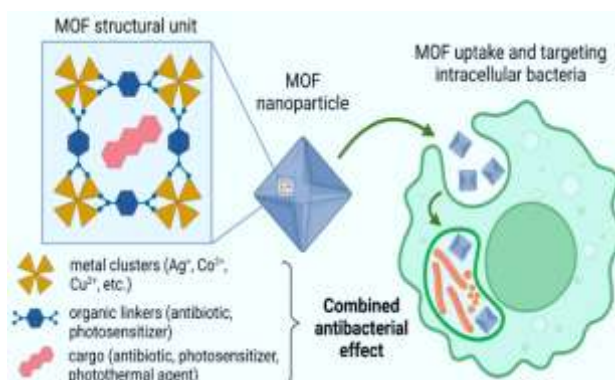


Fig.No.4.1 Drug-bioactive MOF therapy

4.1.2. Drug loaded into a BioMOF

Lin et al. investigated the application of the biocompatible mesoporous iron (Fe^{3+}) terephthalate MOF-53 ($\text{Fe}(\text{OH})[\text{BDC}]$, SBET = $84 \text{ m}^2 \text{ g}^{-1}$, particle size: 500 nm) as DDS for the antibiotic glycopeptide vancomycin (Van) in 2017 [62]. The loaded Van (20 wt%) exhibited a pH-dependent release profile: slower delivery at acidic conditions (pH = 5 vs. pH = 7.4) is associated with higher MOF-53 stability (released Fe^{3+} assessed using inductively coupled plasma atomic emission spectroscopy, ICP-AES). Antimicrobial testing against Gram (+) *S. aureus* revealed that the DDS was efficient, as MOF-53 alone inhibited 30% of the colony forming units (CFU), whereas Van@MOF-53 inhibited 80% (at 100 mg/ml). Bhardwaj, Pandey, and colleagues used physisorption to integrate ampicillin or kanamycin into previously synthesized Zn-based MOFs, IRMOF-3, MOF-5 ($[\text{Zn}_4\text{O}(\text{BDC})_3]$, hydrodynamic size: $2 \times 0.5 \text{ nm}$), and Zn-BTC (crystal needles length: 1-2 mm) [63]. This strategy aimed to combine Zn^{2+} bactericide action with chemotherapy medicines. The characterization of the drug-MOF loaded materials was confined to variations in IRMOF-3@ampicillin particle size measured by dynamic light scattering (DLS), which were most likely caused by the presence of the drug on the MOF's outer surface. Finally, antibacterial testing against Gram (+ve) *S. aureus*, *S. lentus*, *Listeria monocytogenes*, and Gram *Escherichia coli* demonstrated that the bioMOF/drug system outperformed pristine bioMOFs. For all bacteria, the IRMOF₃@ampicillin combination resulted in the lowest minimum inhibitory concentration

(MIC) (100, 50, 50, and 50 mg/ml, respectively). Nonetheless, kinetic tests of the time kill assay revealed that it had equivalent or slightly slower bactericidal effects as the free drug over 24 hours.

Suet al. reported medi-MOF-1 ($\text{Zn}_3(\text{CUR})_{27}(\text{DMA})_3(\text{ethanol})$), a bioMOF DDS. CUR: curcumin: 1,7-bis(4-hydroxy-3-methoxyphenyl) BUs are both AIs: Zn^{2+} and CUR (anti-inflammatory, inhibitor of secreted MDR proteins from cancer cells) [65]. As a model medicine, the anti-inflammatory and analgesic ibuprofen (Ibu) was successfully introduced into the porosity (0.24 gm of drug per g of material). Ibu demonstrated a burst release (40%) in PBS (pH = 7.4, 37°C; measured by UV-vis spectroscopy) within the first hour and then steadily increased to 97% after 80 hours. CUR release and therefore, medi-MOF-1 degradation, exhibited slower kinetics (30% in 1 h) and reached a plateau with 55% of drug release after 24 h, setting the potential use of medi-MOF-1 as co-delivery system of three AIs. In another study, the combination of photodynamic therapy (PDT) of new chlorin-based MOF NPs TBC-Hf and TBP-Hf with the same topology [$\text{Hf}_6(\text{13-O})_4(\text{13 OH})_4(\text{OH})_4(\text{H}_2\text{O})_4(\text{L})_2$] (L = TBC or TBP, H4TBC = 5,10,15,20-tetra(p-benzoate) chlorin, Me4TBP [66]. Creating a crystalline porosity structure based on one or more AIs is a significant difficulty, and the number of bioactive MOFs employed in combination therapy may be limited as a result. novel work on this will most likely be presented in the near future by pushing the limitations of conventional MOF synthesis approaches while also developing novel bioactive chemicals.

4.2. Co-drug delivery from a single MOF

Despite the fact that there are numerous examples of MOF-based DDS [67], they always offer a single loaded medication within the porosity. Nonetheless, the availability of free volume within some MOFs even after encapsulation of a single medication, as well as the advent of one-pot synthetic techniques that allow the encapsulation of bigger molecules surrounded by an outer MOF shell, pave the way for the co-encapsulation of multiple pharmaceuticals. The combination of numerous medications in a single DDS provides significant benefits such as: i) Overcoming various medication pharmacokinetics and cell distribution by coordinating their delivery with a unique DDS, ii) adverse effect reduction resulting from ratiometric drug administration and therapeutic effect enhancement via an additive or synergistic impact, iii) multi-target treatment with a single DDS when the nature of the medicines provides distinct chemotherapy, iv) avoidance and postponement of MDR development by the presence of a medication "cocktail" at the same time, and v) sequential administration via the porosity of the MOF, which is regulated by differences in size and the physicochemical interactions of pharmaceuticals and the MOFs.

The reported study on simultaneous drug loading is quite new, coming only from 2017. For example, Illes et al. MIL-88A, a biocompatible flexible microporous iron (III) fumarate, was proposed for the co-encapsulation of irinotecan (Iri) and floxuridine (FloXu) for the creation of a cancer resistant combination therapy [69]. UV-vis

analysis revealed that the drug capacity was 10.3 wt% Iri (0.103 gg1) and 3.61 wt% Floxu (0.03 gg1). The drugs-loaded material was coated with a lipid seal coating (based on 1,2-dioleoyl-sn-glycero-3-phosphocholine) to avoid premature leaking. Furthermore, cytotoxicity (as measured by the 3-(4,5-dimethylthiazol-2-yl)-2,5-diphenyltetrazolium bromide, MTT tests) was assessed on HeLa cells, with the lowest cell viability (30.6%) when relatively modest dosages (140 mg/ml) were used. Despite this, the IC₅₀ of DDS with a 1:1 Iri:FloXu ratio was higher than that of MIL-88A with just Irri (80 vs. 40 mg/mL). To improve the intracellular uptake of nucleoside reverse transcriptase inhibitors (NRTIs), which are routinely used in anti-HIV (human immunodeficiency virus) therapy, Marcos-Almaraz et al. co-encapsulated two triphosphorylated NRTIs, azidothymidine triphosphate (AZTTP) and lamivudine triphosphate (3TC-Tp), in the biocompatible MIL-100 NPs (SBET = 1500 m² g⁻¹, hydrodynamic size 140 ± 40 nm) [70]. Simultaneous impregnation in water resulted in successful co-loading (6.2 and 3.4 wt% AZT-Tp and 3TCTp, respectively, as measured by HPLC). At 37 °C, in vitro drug co-delivery was examined in PBS supplemented with 10% (w/v) fetal bovine serum (FBS), as well as MOF breakdown by tracking ligand release. 3TC-Tp released quickly (80% in 8 hours), whereas AZT-Tp released gradually over 3 days, which could be attributed to their distinct interactions with the MOF or their size (13×8×4 vs. 12×9×7 Å, respectively).

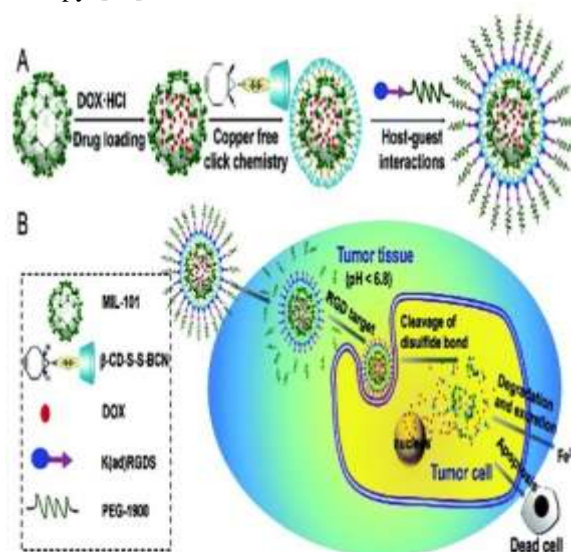


Fig no. 4.2. Co-drug delivery from a single MOF

4.3. Co-encapsulation of a drug and a biomolecule within a single MOF

Other types of active biomolecules could be simultaneously loaded in addition to pharmaceuticals into MOFs for an enhanced bioactive impact and the achievement of a potent and effective combined therapy, in addition to the co-encapsulation of two separate drugs. For instance, He et al. co-encapsulated a cis-platin (CIS) prodrug (proCIS: (cis, cis, trans-[Pt(NH₃)₂Cl₂(OEt)(OCOCH₂-CH₂COOH)]) with small interfering RNA (siRNA) to overcome MDR and re-sensitize ovarian cancer cells towards CIS treatment in the beginning of 2014 [75]. By impregnation, siRNA/UiO-proCIS was created with a proCIS loading of 12 wt%. Confocal fluorescence and the increase in particle size in DLS from 98 to 128 nm from UiO-68-NH₂ to siRNA/UiO-CIS, which is compatible with the presence of some siRNA on the surface, were used to validate the presence of siRNA. Due to the endocytosis intake pathway, cellular absorption of siRNA in ovarian cancer cells (SKOV-3) was enhanced when utilizing MOF as opposed to free siRNA. Additionally, siRNA was gradually administered in PBS (2 mM), producing a 70% content release after 9 h, most likely as a result of the MOF's subsequent decomposition and zirconium's affinity for phosphate. As a result of the synergistic effect of siRNA and CIS co-

delivery, in vitro transfection studies in SKOV-3 revealed that the IC₅₀ of siRNA/UiO-proCIS was 11-fold times lower compared to free proCIS and UiO-proCIS. The down-regulation of MDR expressions and proCIS treatment revealed DNA fragmentation in cells treated with siRNA/UiO-proCIS, indicating that apoptosis was the mechanism of action. The UiO66@AgNCs@Apt@DOX platform described by Su et al. is another illustration of an UiO drug + biomolecule loaded platform [76] Previously created silver nanoclusters (AgNCs) with an AS1411 antigen for an aptamer (Apt) template were ingested simultaneously with DOX inside UiO-66 via one-pot impregnation. DOX release at simulated acidic cancer cell environment (pH = 5) was analysed via UV-vis, obtaining a 60% DOX delivery after 96 h. The potential of the UiO66@AgNCs@Apt@DOX as combined DDS is indicated by the quicker MOF breakdown at pH = 5. A wide concentration range (5–50 gm^l) of the UiO-66@AgNCs@Apt nanocomposite showed poor cytotoxicity against the MCF-7 cell line, and the improved cytotoxicity of UiO-66@AgNCs@Apt@DOX (80%) was attained by the synergistic therapeutic effects of DOX and AS1411 antigen. But it's crucial to note that this combination showed a comparatively high level of cytotoxicity (54%) toward L929 non-carcinogen cells, indicating potential adverse side effects.

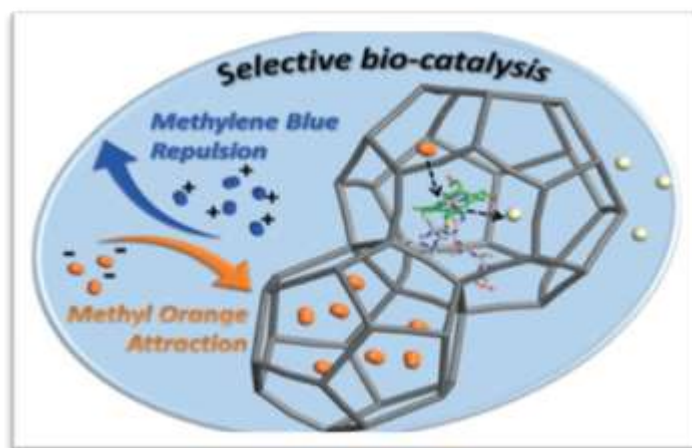


Fig No. 4.3. Co-encapsulation of a drug and a biomolecule within a single MOF

4.4. Co-encapsulation of a drug and an active metal within a single MOF: Chemo- and phototherapy

Sometimes chemotherapy is useless for treating diseases because cells have evolved MDR and co-encapsulating many medications is insufficient. As a result, a synergistic treatment

may be made possible by simultaneously loading other AIs with medications. This strategy has recently been proposed to combat cancer by combining chemotherapy with additional therapeutic modalities, including PTT and PDT [68]. The NIR (which demonstrate low absorption and deep tissue penetration) is converted into heat

(induced hyperthermia) by the excitation of photosensitizers (PS) in kPTT, which causes cellular damage and tumor mitigation. PDT similarly uses PS, but it relies on the production of ROS following radiation to kill cancer cells. Nevertheless, most PS easily aggregate in aqueous solutions. In light of this, their co-encapsulation with pharmaceuticals in MOFs will not only improve their delivery efficacy while increasing PS stability, but also provide a DDS for a combination or synergic therapy. ZIF-8 has been widely utilized as a platform for PTT and chemotherapy. Wang et al. produced a CuS@ZIF-8 core@shell in situ using CuS NPs as PS [65]. By impregnation, DOX was post-synthetically loaded (96 wt%). At pH = 7, no discernible release was seen in PBS, whereas at pH = 5, around 80% of DOX was released after 60 hours. 60% of the DOX in suspensions at pH = 5 was released after just 5 minutes of exposure to NIR. The acceleration in the release kinetics was attributed to the NIR increased ZIF-8 degradation. The CuS@ZIF-8 composite's biocompatibility was demonstrated by cytotoxicity using MCF-7 cells (80% of cell viability at 250 mgmL⁻¹). Less than 20% of the cancer cells were viable with 25 mgmL⁻¹ of CuS + DOX@ZIF-8 (equal to 1 mgmL⁻¹ of loaded DOX) and after NIR irradiation for 6 min, according to an in vitro examination of the synergistic impact. Using photothermal imaging to track the surface temperature following NIR irradiation, the combination of chemo- and PTT was also tested in vivo. A combined chemo- and PTT using ZIF-8 and DOX was similarly proposed by Tian et al., however this time the PS was graphene quantum dots (GQD). The NPs' colloidal stability was verified in PBS for 12 hours with particles ranging in size from 50 to 100 nm [78]. This project is less ambitious than the one before it because the authors looked at the release of DOX at different pH levels (4.55, 6.8, and 7.4) as well as the induction of hyperthermia under NIR radiation of a PBS suspension independently. Additionally, 4T1 cells (mammary cancer) were used only in vitro to investigate the combination of chemo- and PTT. Only 20% of the cells were still alive after posterior irradiation for 3 minutes at 2.5 Wcm² and an 8-hour cell incubation. Cells were examined under a microscope using DOX intrinsic fluorescence, indicating cell amortization and apoptosis following DOX-ZIF-8/GQD therapy. Other recently proposed combined chemo- and PTT DDS uses single Au nanorods (AuNR) inside ZIF-8 (one-pot synthesis) along with DOX (loading 0.358 gg⁻¹) [79]. In physiologically mimicked

settings (PBS, 37⁰C, pH = 5 and 7.4), analysis of the DOX release and NIR photothermal effect revealed that a greater release was attained at pH = 5 after NIR irradiation, with about 100% of drug delivery after 12 h. Parallel to this, writers argued that the released DOX is explained by the ZnO bond breaking with an increase in temperature, taking into account a release of 50% of the total Zn. Although the cancer 4T1 cell line is biocompatible with AuNR@ZIF-8, the synergistic effect of DOX and NIR therapy only produced 10% viability (100 mgmL⁻¹). When 4T1 cells were implanted into mice, in vivo testing showed the ineffectiveness of simply chemotherapy because only 30% of inhibition could be accomplished using AuNR@ZIF-8-DOX. In contrast, the combination of chemo- and PTT induced a 90% tumor suppression. The histology of the heart, liver, spleen, lung, and other major organs of mice subjected to the co-therapy did not alter, indicating no adverse consequences from the treatment. Jiang et al. suggested CuS@ZIF-8-QT (QT: quercetin) as a combination therapy, also based in ZIF-8 and CuS NPs as PS [80]. After analysing the QT delivery following a one-pot synthesis process to produce CuS@ZIF-8-QT, the authors came to the conclusion that adding a protective layer of FA and bovine serum albumin was crucial. CuS@ZIF-8-QT may be used as a combination chemo- and PTT, according to several in vitro investigations (drug release, NIR irradiation, cytotoxicity, and haemolysis). The best efficacy for the combined chemo- and PTT was shown in in vivo antitumor experiments utilizing mice injected with B₁₆F₁₀ as measured by reduction of tumor weight and volume.

4.5. Co-delivery of a drug and a bioactive gas from a single MOF

The combination of medications with physiologically active gases (NO, CO, or H₂S) inside MOF porosity for the treatment of cancer, cardiovascular disorders, and infections is another example of synergic therapy. For instance, CO has been shown to help with wound healing, inflammation, and pro-apoptosis (>250 ppm) in cancer cells in modest doses (100-250 ppm) [88,89]. Its difficult administration at the right concentrations might be overcome with the use of MOFs. Additionally, NO is recognized to be tumor-curing, antimicrobial, and vasodilator. There is a lot of interest in medicinal applications as a result of its encapsulation in various zeolites and MOFs. Increasing immunocompetence,

preventing procarcinogen activation by oxidases, protecting and repairing DNA, and eliminating chronic inflammation are a few other positive benefits of H₂S [81]. Despite the fact that many research have been done on the processes involved in gas storage and delivery in MOFs, as well as the adsorption of gas-releasing molecules as precursors and subsequent gas delivery after an external stimulus [82-84], to the best of our knowledge there are just two works about the simultaneous encapsulation of gas with drugs. The antimetastatic medication Ru(p-cymene) Cl₂(pta) (RAPTA-C, pta: 1,3,5-triaz a-7-phosphaadamantane) was first loaded onto Ni-CPO-27 and released from it as a proof of concept [85]. While RAPTA-C was included by physisorption, NO was chemisorbed. NiCPO-27@RAPTA-C and Ni-CPO-27@RAPTA-C@NO drug release experiments were performed in SBF at 37°C and revealed no discernible difference between NO loaded samples (25% of RAPTA-C was released in 2 h), while NO displayed a burst release under the same

circumstances. To further their understanding, McKinlay et al. combined NO and metronidazole, an antibiotic used to treat a number of parasitic diseases, in Ni-CPO-27 and HKUST-1 in order to examine the impact of MOFs on selectivity, loading capacity, and release [86]. Although Ni-CPO-27 showed a faster release kinetics (100% of the metronidazole was given in 6 h), it had a higher NO loading capacity. The findings showed that there is potential not only for the sequential distribution of AIs but also for regulating the rate of supply by choosing various frameworks. In addition, the antimicrobial activity of both MOFs against *P. aeruginosa* and *S. aureus* was evaluated. Different controls showed that a single dose of metronidazole did not significantly reduce bacterial growth when compared to pristine MOF, most likely due to the restricted release of MOF ions through the closed pores. The effectiveness of the synergistic therapy was demonstrated by the quick bactericidal activity of both MOF platforms when metronidazole and NO were co-encapsulated.



Fig No. 4.5. Co-delivery of a drug and a bioactive gas from a single MOF.

V. TOXICITY ASPECTS OF MOFS

The toxicity issue with this adaptable carrier is receiving a lot of attention along with the increased interest in research on MOFs and nano MOFs. The toxicity of this substance is still a major concern even though it has distinct features, a large surface area, and can be altered in terms of size, shape, and composition. MOFs with metal counterparts, such as those with iron and zirconium bases, have already been investigated for potential toxicity, and the same has been determined in these cases [87]. However, because they influence the rate of breakdown, the manufacturing technique, elemental content, and size of MOFs may also affect their toxicity. There have been research on the toxicity of MOFs, despite the fact that they are

rare in number. Other factors that can affect toxicity besides MOF size and form are the type of linker used, the surface-modifying agent used, and the type of metal used. The literature published on the toxicity aspects of MOFs gives contradictory inferences [96]. NanoZIF-8, which has a size of about 200 nm, was tested against malignant cell lines in a study, including promyelocytic leukaemia [HL-60], colorectal adenocarcinoma [HT-29], and mucoepidermoid carcinoma of the lung [NCI-H₂₉₂]. The results demonstrated the absence of any toxicity even at a concentration of 109 M [88]. Similar research on the effects of nanoZIF-8's toxicity on HeLa and J774 cells found that the cytotoxicity IC₅₀ values were 436 and 109 M, respectively [89]. Additionally, HepG2 and MCF7

cells were used to test the toxicity of nano MOFs. The findings showed that toxicity varied with MOF solubility. These results were also supported by *in vivo* against zebrafish embryos [90]. As was previously mentioned, although a number of factors, including size, shape, morphology, and solvent type, affect how toxic MOFs are, the main variables that have a significant impact on how toxic MOFs are are the metal ions used, the kinds of organic linkers used, and the kinds of solvents used to synthesize MOFs.

The type of metal used in MOFs is an area of concern when it comes to toxicity. Iron, zinc, copper-cobalt, zirconium, cadmium, nickel, and other transition metals are the most widely employed metal ions in MOFs [91]. Although other metal ions are being studied, such as gallium and titanium, this research is still in its early stages. Due to their biological usage in the body, iron and copper among these metals have the lowest toxicity, whereas cadmium has the highest toxicity risk. While iron ions induce short-term oxidative damage in the liver and spleen and the remaining iron is metabolized and expelled in urine and feces, carboxylate linker is immediately eliminated from animals through their urine and feces [92]. There is a potential that the metal ions will oxidize, which could harm the cells. The safer metals that can be used in MOFs include Mg^{2+} ($LD_{50} MgSO_4 = 5000$), Ca^{2+} ($LD_{50} CaCl_2 = 1940$), Fe^{3+} ($LD_{50} FeCl_3 = 450$), Fe^{2+} ($LD_{50} FeCl_2 = 984$), and Zn^{2+} ($LD_{50} Zn(OAc)_2 = 100-600$), which have lower lethal doses upon oral administration [93]. In addition to the metals described above, biologically inert cations such as gold, silver, zirconium, and titanium could be used to synthesize biocompatible MOFs [94].

For the synthesis of MOFs, a variety of linkers including carboxylates, phosphonates, sulfonates, imidazolates, phenolates, and amines have been investigated. There aren't many reports on toxicity investigations on these linkers, and there isn't much toxicity profiling. Several publications claim that exposure to these linkers is directly linked to a number of health problems. A few linkers, such as terephthalic acid, might produce minor respiratory tract irritation as well as irritation of the lips, eyes, nose, and skin when exposed [95]. Similarly, long term exposure to trimesic acid irritates the eyes and skin.

The toxicity of the solvents utilized in the synthesis of MOFs has also been investigated. The presence of chloroform in MOFs after synthesis has negative consequences on human health, producing hepatic and renal toxicity in numerous species,

according to published literature. Oral ingestion of chloroform solution results in immediate hypoventilation, transitory hypotension, and instantaneous unconsciousness in addition to hepatic and renal damage. Similar to this, when MOFs are produced using dimethylformamide (DMF), short-term exposure may cause rashes, alcohol intolerance, nausea, vomiting, jaundice, and abdominal pain, while long-term exposure may cause liver damage and other negative health effects. In the instance of acetone-mediated MOF production, acetone's presence in MOFs can cause cutaneous and ocular irritation at modest doses, while a severe exposure can also cause neurotoxicity or irritation of the respiratory tract.

Recent research has shown that the surface properties of MOFs also affect their toxicity. It is generally known that the surface characteristics influence how nanoparticles interact with different body parts. Similar to this, the MOF's interaction with biological molecules and fluids depends heavily on its surface characteristics. In comparison to uncoated MIL-100(Fe), research employing heparin-coated MIL-100(Fe) that was produced using $[Fe_3OH(H_2O)_2(BTC)_2]$, H_3BTC , and trimesic acid showed reduced cell recognition, complement activation, and reactive oxygen generation.

VI. CHALLENGES AND PROSPECTS FOR TRANSLATIONAL MEDICAL APPLICATIONS OF NMOFS

6.1. Considerable Advances

The development of NMOFs as drug nanocarriers, molecular imaging probes, and theranostic systems has garnered much attention for biomedical applications due to their large surface area, tunable pore size and shape, adjustable composition and structure, inherent biodegradability, versatile functionality, and mild synthetic conditions. First, a number of preparation methods have been created to mildly synthesize NMOFs with a variety of sizes and morphologies, high yields, and high purity. Secondly, NMOFs have exhibited high loading capacity for therapeutic molecules. NMOFs have been effectively used to encapsulate a variety of medicinal substances, including neutral and ionic medicines, proteins, and genes. In most cases, the controlled release of loaded therapeutic agents was demonstrated. Third, a lot of NMOFs have been researched as molecular imaging probes for MR and optical imaging in biomedicine. Personalized patient care is now available thanks to NMOFs'

high loading capacities and promising theranostic nanoplatform capabilities.

6.2. Challenges and Prospects

Despite the previous ten years' substantial advancements in NMOFs, there are still certain obstacles before these materials can be used in clinical settings. First and foremost, the toxicity and biocompatibility of NMOFs require much more research. The finest organic linkages would be those that are endogenous organic spacers and constituent parts of the body since they may lower the likelihood of negative effects. In addition, the direct introduction of therapeutic molecules as organic links is also a good choice. The translation of the vast number of NMOFs that are now being produced into the clinic will be facilitated by a thorough understanding of molecular characteristics, biodistribution, and targeting mechanisms. Secondly, much effort should be devoted to the stability and surface modification of NMOFs. A certain level of chemical instability is required for NMOFs to function as nanocarriers of therapeutic compounds, not only because drug release efficiency is affected by drug degradation, but also because the body's own mechanisms may be able to deal with the degradation products to prevent endogenous build up. However, the degradation mechanism of currently available NMOFs requires further study. However, because NMOFs must be stable and soluble in water for biological application, surface modification of NMOFs with ligands is also a significant issue. Such modification can extend the blood circulation half-life, improve drug delivery effectiveness, and provide targeting capabilities. However, to date, studies on the surface modification of NMOFs have been very limited. Thirdly, research on theranostic and molecular imaging applications of NMOFs is still far from clinical testing and must address a number of difficulties, such as the discrepancy between the optimum doses of therapeutic and imaging agents in such applications. Prior to clinical translation, improved NMOF performance requires more systematic in vivo research, including studies of the best administration methods.

VII. CONCLUSION

Significant progress has been made in adapting MOFs and NMOFs for drug delivery. These hybrid systems allow for the precise assembly and customization of a huge number of metal centers and organic building blocks to create

novel materials with desirable properties as drug carriers. NMOFs are an infinitely adjustable material platform, so in the near future, a lot more pharmaceuticals will be put into them. The efficacy investigations of this potential class of nanotherapeutics should be substantially facilitated by the capacity to transport both imaging and therapeutic chemicals in NMOFs. MOFs and NMOFs have a promising future in drug delivery, but significant advancements must be made before they can be used in clinical settings.

Given that MOF safety must be taken into account in biomedical and pharmaceutical applications, particular attention must be paid to certain factors like composition, particle size, and stability under particular biorelevant conditions. Despite the growing body of in vitro and in vivo research on MOF biocompatibility, there is still a dearth of toxicological data regarding MOFs that must be systematically and thoroughly addressed while taking into account the target application (e.g., relevant circumstances, biodistribution, accumulation, metabolism, bioelimination, administration route).

It is anticipated that MOFs will be crucial in the future development of multifunctional tailored medicines and/or diagnosis due to their incredibly adaptable nature. On the other hand, significant progress is now developing fast in conferring targeting abilities to MOFs. Theragnosis and targeting are further combined within a MOF structure, outlining the promising future of these materials in the biomedical industry. The diversification on MOFs bio applications will continue and other combined treatments will be probably explored soon.

REFERENCES

- [1]. C.T. Keith, A.A. Borisy, B.R. Stockwell, Multicomponent therapeutics for networked systems, *Nat. Rev. Drug Discover.* 4 (2005) 71–78, <https://doi.org/10.1038/nrd1609>.
- [2]. W.G. Kaelin, The concept of synthetic lethality in the context of anticancer therapy, *Nat. Rev. Cancer* 5 (2005) 689–698, <https://doi.org/10.1038/nrc1691>.
- [3]. J.R. Sharom, D.S. Bellows, M. Tyers, From large networks to small molecules, *Curr. Opin. Chem. Biol.* 8 (2004) 81–90, <https://doi.org/10.1016/j.cbpa.2003.12.007>.
- [4]. J.H. Ryu, H. Koo, I.-C. Sun, S.H. Yuk, K. Choi, K. Kim, I.C. Kwon, Tumor-

- targeting multi-functional nanoparticles for theragnosis: new paradigm for cancer therapy, *Adv. Drug Deliv. Rev.* 64 (2012) 1447–1458, <https://doi.org/10.1016/j.addr.2012.06.012>.
- [5]. Li H, Eddaoudi M, O’Keeffe M, Yaghi OM: Design and synthesis of an exceptionally stable and highly porous metal–organic framework. *Nature* 1999, 402:276-279.
- [6]. Evans OR, Xiong R-G, Wang Z, Wong GK, Lin W: Crystal engineering of acentric diamondoid metal–organic coordination networks. *Angew Chem Int Ed* 1999, 38:536-538.
- [7]. Moulton B, Zaworotko MJ: From molecules to crystal engineering: supramolecular isomerism and polymorphism in network solids. *J Chem Rev* 2001, 101:1629-1658.
- [8]. Kitagawa S, Kitaura R, Noro S-I: Functional porous coordination polymers. *Angew Chem Int Ed* 2004, 43:2334-2375.
- [9]. Oh M, Mirkin CA: Chemically tailorable colloidal particles from infinite coordination polymers. *Nature* 2005, 438:651-654.
- [10]. Evans OR, Lin W: Crystal engineering of NLO materials based on metal–organic coordination networks. *Acc Chem Res* 2002, 35:511-522.
- [11]. Seo JS, Whang D, Lee H, Jun SI, Oh J, Jeon YJ, Kim K: A homochiral metal–organic porous material for enantioselective separation and catalysis. *Nature* 2000, 404:982-986.
- [12]. Ferey G, Latroche M, Serre C, Millange F, Loiseau T, PercheronGuegan A: Hydrogen adsorption in the nanoporous metalbenzenedicarboxylate $M(OH)(O_2C-C_6H_4-CO_2)$ ($M = Al^{3+}, Cr^{3+}$), MIL-53. *Chem Commun* 2003:2976-2977.
- [13]. Chen B, Wang L, Xiao Y, Fronczek FR, Xue M, Cui Y, Qian G: A luminescent metal–organic framework with Lewis basic pyridyl sites for the sensing of metal ions. *Angew Chem Int Ed* 2009, 48:500-503.
- [14]. Lan A, Li K, Wu H, Olsson DH, Emge TJ, Ki W, Hong M, Li J: A luminescent microporous metal–organic framework for the fast and reversible detection of high explosives. *Angew Chem Int Ed* 2009, 48:2334-233819.
- [15]. Lin W, Wang L, Ma L: A novel octupolar metal–organic NLO material based on a chiral 2D coordination network. *J Am Chem Soc* 1999, 121:11249-11250.
- [16]. Park KH, Jang K, Son SU, Sweigart DA: Self-supported organometallic rhodium quinonoid nano catalysts for stereoselective polymerization of phenylacetylene. *J Am Chem Soc* 2006, 128:8740-8741.
- [17]. Rieter WJ, Taylor KML, Lin W: Surface modification and functionalization of nanoscale metal–organic frameworks for controlled release and luminescence sensing. *J Am Chem Soc* 2007, 129:9852-9853
- [18]. Rieter WJ, Taylor KML, An H, Lin W, Lin W: Nanoscale metal– organic frameworks as potential multimodal contrast enhancing agents.
- [19]. Taylor KML, Rieter WJ, Lin W: Manganese-based nanoscale metal–organic frameworks for magnetic resonance imaging. *J Am Chem Soc* 2008, 130:14358-14359.
- [20]. Taylor KML, Jin A, Lin W: Surfactant-assisted synthesis of nanoscale gadolinium metal–organic frameworks for potential multimodal imaging. *Angew Chem Int Ed* 2008, 47:7722-7725.
- [21]. deKrafft KE, Xie Z, Cao G, Tran S, Ma L, Zhou OZ, Lin W: Iodinated nanoscale coordination polymers as potential contrast agents for computed tomography. *Angew Chem Int Ed* 2009, 48:9901-9904.
- [22]. V.V. Butova, M.A. Soldatov, A.A. Guda, K.A. Lomachenko, C. Lamberti, Metalorganic frameworks: structure, properties, methods of synthesis and characterization, *Russ. Chem. Rev.* 85 (2016) 280, <https://doi.org/10.1070/RCR4554>.
- [23]. D.J. Tranche Montagne, J.R. Hunt, O.M. Yaghi, Room temperature synthesis of metal-organic frameworks: MOF-5, MOF-74, MOF-177, MOF-199, and IRMOF-0, *Tetrahedron* 64 (2008) 8553–8557, <https://doi.org/10.1016/j.tet.2008.06.036>.
- [24]. L. Huang, H. Wang, J. Chen, Z. Wang, J. Sun, D. Zhao, Y. Yan, Synthesis, morphology control, and properties of porous metal–organic coordination polymers, *Microporous Mesoporous*

- Mater. 58 (2003) 105–114, [https://doi.org/10.1016/S1387-1811\(02\)00609-1](https://doi.org/10.1016/S1387-1811(02)00609-1).
- [25]. K.S. Park, Z. Ni, A.P. Côté, J.Y. Choi, R. Huang, F.J. Uribe-Romo, H.K. Chae, M. O’Keeffe, O.M. Yaghi, Exceptional chemical and thermal stability of zeolitic imidazolate frameworks, PNAS 103 (2006) 10186–10191, <https://doi.org/10.1073/pnas.0602439103>.
- [26]. J. Cravillon, S. Münzer, S.-J. Lohmeier, A. Feldhoff, K. Huber, M. Wiebcke, Rapid room-temperature synthesis and characterization of nanocrystals of a prototypical zeolitic imidazolate framework, Chem. Mater. 21 (2009) 1410–1412, <https://doi.org/10.1021/cm900166h>.
- [27]. X.-C. Huang, Y.-Y. Lin, J.-P. Zhang, X.-M. Chen, Ligand-directed strategy for zeolite-type metal-organic frameworks: zinc (II) imidazolates with unusual zeolitic topologies, Angew. Chem. Int. Ed. Engl. 45 (2006) 1557–1559, <https://doi.org/10.1002/anie.200503778>.
- [28]. J. Li, S. Cheng, Q. Zhao, P. Long, J. Dong, Synthesis and hydrogen-storage behaviour of metal–organic framework MOF-5, Int. J. Hydrogen Energy 34 (2009) 1377–1382, <https://doi.org/10.1016/j.ijhydene.2008.11.048>.
- [29]. S.-H. Jung, J.-H. Lee, J.-S. Chang, Microwave synthesis of a nanoporous hybrid material, chromium trimesate, Bull. Korean Chem. Soc. 26 (2005) 880–881, <https://doi.org/10.5012/bkcs.2005.26.6.880>.
- [30]. G. Férey, C. Serre, C. Mellot-Draznieks, F. Millange, S. Surblé, J. Dutour, I. Margiolaki, A hybrid solid with giant pores prepared by a combination of targeted chemistry, simulation, and powder diffraction, Angew. Chem. Int. Ed. Engl. 43 (2004) 6296–6301, <https://doi.org/10.1002/anie.200460592>.
- [31]. K.M.L. Taylor-Pashow, J. Della Rocca, Z. Xie, S. Tran, W. Lin, Post synthetic modifications of iron-carboxylate nanoscale metal organic frameworks for imaging and drug delivery, J. Am. Chem. Soc. 131 (2009) 14261–14263, <https://doi.org/10.1021/ja906198y>.
- [32]. S.H. Jung, J.-H. Lee, J.W. Yoon, C. Serre, G. Férey, J.-S. Chang, Microwave synthesis of chromium terephthalate MIL-101 and its benzene sorption ability, Adv. Mater. 19 (2007) 121–124, <https://doi.org/10.1002/adma.200601604>.
- [33]. N.A. Khan, I.J. Kang, H.Y. Seok, S.H. Jung, Facile synthesis of nano-sized metal-organic frameworks, chromium-benzene dicarboxylate, MIL-101, Chem. Eng. J. 166 (2011) 1152–1157, <https://doi.org/10.1016/j.cej.2010.11.098>.
- [34]. Y.-K. Seo, G. Hundal, I.T. Jang, Y.K. Hwang, C.-H. Jun, J.-S. Chang, Microwave synthesis of hybrid inorganic–organic materials including porous Cu₃(BTC)₂ from Cu (II)-trimesate mixture, Microporous Mesoporous Mater. 119 (2009) 331–337, <https://doi.org/10.1016/j.micromeso.2008.10.035>.
- [35]. U. Mueller, M. Schubert, F. Teich, H. Puetter, K. Schierle-Arndt, J. Pastré, Metal–organic frameworks—prospective industrial applications, J. Mater. Chem. 16 (2006) 626–636, <https://doi.org/10.1039/B511962F>.
- [36]. M. Schlesinger, S. Schulze, M. Hietschold, M. Mehring, Evaluation of synthetic methods for microporous metal–organic frameworks exemplified by the competitive formation of [Cu₂(btc)₃(H₂O)₃] and [Cu₂(btc)(OH)(H₂O)], Microporous Mesoporous Mater. 132 (2010) 121–127, <https://doi.org/10.1016/j.micromeso.2010.02.008>.
- [37]. R. Ameloot, L. Stappers, J. Fransaer, L. Alaerts, B.F. Sels, D.E. De Vos, Patterned growth of metal-organic framework coatings by electrochemical synthesis, Chem. Mater. 21 (2009) 2580–2582, <https://doi.org/10.1021/cm900069f>.
- [38]. R. Ameloot, L. Pandey, M.V. der Auweraer, L. Alaerts, B.F. Sels, D.E.D. Vos, patterned film growth of metal–organic frameworks based on galvanic displacement, Chem. Commun. 46 (2010) 3735–3737, <https://doi.org/10.1039/C001544J>.
- [39]. L.-G. Qiu, Z.-Q. Li, Y. Wu, W. Wang, T. Xu, X. Jiang, Facile synthesis of nanocrystals of a microporous metal–organic framework by an ultrasonic method and selective sensing of organ amines, Chem. Commun. (2008) 3642–3644, <https://doi.org/10.1039/B804126A>.

- [40]. W.-J. Son, J. Kim, J. Kim, W.-S. Ahn, Sonochemical synthesis of MOF-5, *Chem. Commun.* (2008) 6336–6338, <https://doi.org/10.1039/B814740J>.
- [41]. R. Sabouni, H. Kazemian, S. Rohani, A novel combined manufacturing technique for rapid production of IRMOF-1 using ultrasound and 44 microwave energies, *Chem. Eng. J.* 165 (2010) 966–973, <https://doi.org/10.1016/j.cej.2010.09.036>.
- [42]. Z.-Q. Li, L.-G. Qiu, T. Xu, Y. Wu, W. Wang, Z.-Y. Wu, X. Jiang, Ultrasonic synthesis of the microporous metal–organic framework Cu₃(BTC)₂ at ambient temperature and pressure: an efficient and environmentally friendly method, *Mater. Lett.* 63 (2009) 78–80, <https://doi.org/10.1016/j.matlet.2008.09.010>.
- [43]. N.A. Khan, S.-H. Jung, Facile syntheses of metal-organic framework Cu₃(BTC)₂(H₂O)₃ under ultrasound, *Bull. Korean Chem. Soc.* 30 (2009) 2921–2926, <https://doi.org/10.5012/bkcs.2009.30.12.2921>.
- [44]. N.A. Khan, M.M. Haque, S.H. Jung, Accelerated syntheses of porous isostructural lanthanide-benzene tricarboxylates (Ln–BTC) under ultrasound at room temperature, *Eur. J. Inorg. Chem.* 2010 (2010) 4975–4981, <https://doi.org/10.1002/ejic.201000541>.
- [45]. D.-W. Jung, D.-A. Yang, J. Kim, J. Kim, W.-S. Ahn, Facile synthesis of MOF-177 by a sonochemical method using 1-methyl-2-pyrrolidinone as a solvent, *Dalton Trans.* 39 (2010) 2883–2887, <https://doi.org/10.1039/B925088C>.
- [46]. J. Kim, S.-T. Yang, S.B. Choi, J. Sim, J. Kim, W.-S. Ahn, Control of catenation in CuTATB-n metal–organic frameworks by sonochemical synthesis and its effect on CO₂ adsorption, *J. Mater. Chem.* 21 (2011) 3070–3076, <https://doi.org/10.1039/C0JM03318A>.
- [47]. A.L. Garay, A. Pichon, S.L. James, Solvent-free synthesis of metal complexes, *Chem. Soc. Rev.* 36 (2007) 846–855, <https://doi.org/10.1039/B600363J>.
- [48]. W. Yuan, T. Friscić, D. Apperley, S.L. James, High reactivity of metal-organic frameworks under grinding conditions: parallels with organic molecular materials, *Angew. Chem. Int. Ed. Engl.* 49 (2010) 3916–3919, <https://doi.org/10.1002/anie.200906965>.
- [49]. T. Friscić, D.G. Reid, I. Halasz, R.S. Stein, R.E. Dinnebier, M.J. Duer, Ion- and liquid-assisted grinding: improved mechanochemical synthesis of metalorganic frameworks reveals salt inclusion and anion templating, *Angew. Chem. Int. Ed. Engl.* 49 (2010) 712–715, <https://doi.org/10.1002/anie.200906583>.
- [50]. A. Pichon, A. Lazuen-Garay, S.L. James, Solvent-free synthesis of a microporous metal–organic framework, *CrystEngComm* 8 (2006) 211–214, <https://doi.org/10.1039/B513750K>.
- [51]. A. Pichon, S.L. James, An array-based study of reactivity under solvent-free mechanochemical conditions—insights and trends, *CrystEngComm* 10 (2008) 1839–1847, <https://doi.org/10.1039/B810857A>.
- [52]. P.J. Beldon, L. Fábíán, R.S. Stein, A. Thirumurugan, A.K. Cheetham, T. Frišćić, Rapid room-temperature synthesis of zeolitic imidazolate frameworks by using mechanochemistry, *Angew. Chem. Int. Ed. Engl.* 49 (2010) 9640–9643, <https://doi.org/10.1002/anie.201005547>.
- [53]. McKinlay AC, Morris RE, Horcajada P, et al. BioMOFs: metal–organic frameworks for biological and medical applications. *Angew Chem Int Ed* 2010; 49:6260-6.
- [54]. Horcajada P, Serre C, Vallet-Reg M, et al. Metal–organic frameworks as efficient materials for drug delivery. *Angew Chem Int Ed* 2006; 45:5974-8.
- [55]. Horcajada P, Serre C, Maurin G, et al. Flexible porous metal-organic frameworks for a controlled drug delivery. *J Am Chem Soc* 2008; 130:6774-80.
- [56]. Sun CY, Qin C, Wang XL, et al. Zeolitic imidazolate framework-8 as efficient pH-sensitive drug delivery vehicle. *Dalton Trans* 2012; 41:6906-9.
- [57]. P. Horcajada, R. Gref, T. Baati, P.K. Allan, G. Maurin, P. Couvreur, Metal Organic Frameworks in Biomedicine, in: *Met. Fram. Appl. from Catal. to Gas Storage*, 2012, pp. 1232–1268.
- [58]. J. Mehta, N. Bhardwaj, S.K. Bhardwaj, K.H. Kim, A. Deep, Recent advances in

- enzyme immobilization techniques: Metal-organic frameworks as novel substrates, *Coord. Chem. Rev.* 322 (2016) 30–40, <https://doi.org/10.1016/j.ccr.2016.05.007>.
- [59]. C. Rösler, R.A. Fischer, Metal-organic frameworks as hosts for nanoparticles, *CrystEngComm* 17 (2015) 199–217, <https://doi.org/10.1039/C4CE01251H>.
- [60]. S.R. Miller, D. Heurtaux, T. Baati, P. Horcajada, J.-M. Grenèche, C. Serre, Biodegradable therapeutic MOFs for the delivery of bioactive molecules, *Chem. Commun.* 46 (2010) 4526, <https://doi.org/10.1039/c001181a>.
- [61]. C. Tamames-Tabar, E. Imbuluzqueta, N. Guillou, C. Serre, S.R. Miller, E. Elkaïm, P. Horcajada, M.J. Blanco-Prieto, A Zn azelate MOF: combining antibacterial effect, *CrystEngComm* 17 (2015) 456–462, <https://doi.org/10.1039/C4CE00885E>.
- [62]. S. Lin, X. Liu, L. Tan, Z. Cui, X. Yang, K.W.K. Yeung, H. Pan, S. Wu, Porous iron carboxylate metal-organic framework: a novel bio platform with sustained antibacterial efficacy and nontoxicity, *ACS Appl. Mater. Interfaces* 9 (2017) 19248–19257, <https://doi.org/10.1021/acsami.7b04810>.
- [63]. N. Bhardwaj, S.K. Pandey, J. Mehta, S.K. Bhardwaj, K.-H. Kim, A. Deep, Bioactive nano-metal-organic frameworks as antimicrobials against Gram-positive and Gram-negative bacteria, *Toxicol. Res. (Camb)* 7 (2018) 931–941, <https://doi.org/10.1039/C8TX00087E>.
- [64]. D.J. Levine, T. Runc̃evski, M.T. Kapelewski, B.K. Keitz, J. Oktawiec, D.A. Reed, J. A. Mason, H.Z.H. Jiang, K.A. Colwell, C.M. Legendre, S.A. FitzGerald, J.R. Long, Olsalazine-based metal-organic frameworks as biocompatible platforms for H₂ adsorption and drug delivery, *J. Am. Chem. Soc.* 138 (2016) 10143–10150, <https://doi.org/10.1021/jacs.6b03523>.
- [65]. H. Su, F. Sun, J. Jia, H. He, A. Wang, G. Zhu, A highly porous medical metal-organic framework constructed from bioactive curcumin, *Chem. Commun.* 51 (2015) 5774–5777, <https://doi.org/10.1039/C4CC10159F>.
- [66]. K. Lu, C. He, N. Guo, C. Chan, K. Ni, R.R. Weichselbaum, W. Lin, Chlorin-based nanoscale metal-organic framework systemically rejects colorectal cancers via synergistic photodynamic therapy and checkpoint blockade immunotherapy, *J. Am. Chem. Soc.* 138 (2016) 12502–12510, <https://doi.org/10.1021/jacs.6b06663>.
- [67]. L. Wang, M. Zheng, Z. Xie, Nanoscale metal-organic frameworks for drug delivery: a conventional platform with new promise, *J. Mater. Chem. B* 6 (2018) 707–717, <https://doi.org/10.1039/C7TB02970E>.
- [68]. J.-Y. Zeng, X.-S. Wang, W.-F. Song, H. Cheng, X.-Z. Zhang, Metal-organic framework mediated multifunctional nanoplatforams for cancer therapy, *Adv. Therp.* 2 (2019), <https://doi.org/10.1002/adtp.201800100>, 1800100.
- [69]. B. Illes, S. Wuttke, H. Engelke, Liposome-coated iron fumarate metal-organic framework nanoparticles for combination therapy, *Nanomaterials* 7 (2017) 351, <https://doi.org/10.3390/nano7110351>.
- [70]. M.T. Marcos-Almaraz, R. Gref, V. Agostoni, C. Kreuz, P. Clayette, C. Serre, P. Couvreur, P. Horcajada, Towards improved HIV-microbicide activity through the co-encapsulation of NRTI drugs in biocompatible metal organic framework nanocarriers, *J. Mater. Chem. B* 5 (2017) 8563–8569, <https://doi.org/10.1039/C7TB01933E>.
- [71]. F.-M. Zhang, H. Dong, X. Zhang, X.-J. Sun, M. Liu, D.-D. Yang, X. Liu, J.-Z. Wei, Post synthetic modification of ZIF-90 for potential targeted codelivery of two anticancer drugs, *ACS Appl. Mater. Interfaces* 9 (2017) 27332–27337, <https://doi.org/10.1021/acsami.7b08451>.
- [72]. H. Zhang, W. Jiang, R. Liu, J. Zhang, D. Zhang, Z. Li, Y. Luan, Rational design of metal organic framework nanocarrier-based codelivery system of doxorubicin hydrochloride/verapamil hydrochloride for overcoming multidrug resistance with efficient targeted cancer therapy, *ACS Appl. Mater. Interfaces* 9 (2017) 19687–19697, <https://doi.org/10.1021/acsami.7b05142>.

- [73]. L. Wang, H. Guan, Z. Wang, Y. Xing, J. Zhang, K. Cai, Hybrid mesoporous microporous nanocarriers for overcoming multidrug resistance by sequential drug delivery, *Mol. Pharm.* 15 (2018) 2503–2512, <https://doi.org/10.1021/acs.molpharmaceut.7b01096>.
- [74]. L. Zhang, Z. Wang, Y. Zhang, F. Cao, K. Dong, J. Ren, X. Qu, Erythrocyte membrane cloaked metal-organic framework nanoparticle as biomimetic nanoreactor for starvation-activated colon cancer therapy, *ACS Nano* 12 (2018) 10201–10211, <https://doi.org/10.1021/acsnano.8b05200>.
- [75]. C. He, K. Lu, D. Liu, W. Lin, Nanoscale Metal Organic Frameworks for the codelivery of cisplatin and Pooled siRNAs to enhance therapeutic efficacy in drug-resistant ovarian cancer cell, *J. Am. Chem. Soc.* 136 (2014) 5181–5184, <http://pubs.acs.org/doi/pdf/10.1021/ja4098862>.
- [76]. F. Su, Q. Jia, Z. Li, M. Wang, L. He, D. Peng, Y. Song, Z. Zhang, S. Fang, Aptamer templated silver nanoclusters embedded in zirconium metal-organic framework for targeted antitumor drug delivery, *Microporous Mesoporous Mater.* 275 (2019) 152–162, <https://doi.org/10.1016/j.micromeso.2018.08.026>.
- [77]. Y. Zhang, F. Wang, E. Ju, Z. Liu, Z. Chen, J. Ren, X. Qu, Metal-organic framework-based vaccine platforms for enhanced systemic immune and memory response, *Adv. Funct. Mater.* 26 (2016) 6454–6461, <https://doi.org/10.1002/adfm.201600650>.
- [78]. Y. Yang, Q. Chen, J.-P. Wu, T.B. Kirk, J. Xu, Z. Liu, W. Xue, Reduction-responsive codelivery system based on a metal-organic framework for eliciting potent cellular immune response, *ACS Appl. Mater. Interfaces* 10 (2018) 12463–12473, <https://doi.org/10.1021/acsami.8b01680>.
- [79]. S.K. Alsaiani, S. Patil, M. Alyami, K.O. Alamoudi, F.A. Aleisa, J.S. Merzaban, M. Li, N.M. Khashab, Endosomal escape and delivery of CRISPR/Cas9 genome editing machinery enabled by nanoscale zeolitic imidazolate framework, *J. Am. Chem. Soc.* 140 (2018) 143–146, <https://doi.org/10.1021/jacs.7b11754>.
- [80]. T.T. Chen, J.T. Yi, Y.Y. Zhao, X. Chu, Biomaterialized metal-organic framework nanoparticles enable intracellular delivery and endo-lysosomal release of native active proteins, *J. Am. Chem. Soc.* 140 (2018) 9912–9920, <https://doi.org/10.1021/jacs.8b04457>.
- [81]. Z. Wang, X. Tang, X. Wang, D. Yang, C. Yang, Y. Lou, J. Chen, N. He, Near infrared light-induced dissociation of zeolitic imidazole framework-8 (ZIF-8) with encapsulated CuS nanoparticles and their application as a therapeutic nanoplatform, *Chem. Commun.* 52 (2016) 12210–12213, <https://doi.org/10.1039/C6CC06616J>.
- [82]. Z. Tian, X. Yao, K. Ma, X. Niu, J. Grothe, Q. Xu, L. Liu, S. Kaskel, Y. Zhu, Metalorganic framework/graphene quantum dot nanoparticles used for synergistic chemo- and photothermal therapy, *ACS Omega* 2 (2017) 1249–1258, <https://doi.org/10.1021/acsomega.6b00385>.
- [83]. Y. Li, J. Jin, D. Wang, J. Lv, K. Hou, Y. Liu, C. Chen, Z. Tang, Coordination responsive drug release inside gold nanorod@metal-organic framework core-shell nanostructures for near-infrared-induced synergistic chemo photothermal therapy, *Nano Res.* 11 (2018) 3294–3305, <https://doi.org/10.1007/s12274-017-1874-y>.
- [84]. W. Jiang, H. Zhang, J. Wu, G. Zhai, Z. Li, Y. Luan, S. Garg, CuS@MOF-Based well designed quercetin delivery system for chemo-photothermal therapy, *ACS Appl. Mater. Interfaces* 10 (2018) 34513–34523, <https://doi.org/10.1021/acsami.8b13487>.
- [85]. J.-C. Yang, Y. Chen, Y.-H. Li, X.-B. Yin, Magnetic resonance imaging-guided multi-drug chemotherapy and photothermal synergistic therapy with pH and NIR-stimulation release, *ACS Appl. Mater. Interfaces* 9 (2017) 22278–22288, <https://doi.org/10.1021/acsami.7b06105>.
- [86]. Y.-D. Da Zhu, S.-P. Chen, H. Zhao, Y. Yang, X.-Q. Chen, J. Sun, H.-S. Fan, X.-D. Zhang, PPy@MIL-100 nanoparticles as a pH- and near-IR-irradiation responsive drug carrier for simultaneous photothermal therapy and chemotherapy



- of cancer cells, ACS Appl. Mater. Interfaces 8 (2016) 34209– 34217, <https://doi.org/10.1021/acsami.6b11378>.
- [87]. J.-Y. Zeng, M.-K. Zhang, M.-Y. Peng, D. Gong, X.-Z. Zhang, Porphyrinic metalorganic frameworks coated gold nanorods as a versatile nanoplatform for combined photodynamic/photothermal/chemotherapy of tumor, Adv. Funct. Mater. 28 (2018) 1705451, <https://doi.org/10.1002/adfm.201705451>.